University College London

Literature Survey and Outline

Understanding Cosmic Muons Through Simulation

PHAS0097 - MSci Physics Project

Hugo Neely

First Supervisor: Dr Andreas Korn

Second Supervisor: Prof Ryan Nichol

Word count: 2483

1st November 2021

Contents

1 Background

1.1 Muon physics

Muons are elementary particles often referred to as heavier siblings of the electron. Muons and electrons belong to the same family of subatomic particles (leptons) and so interact very similarly in many respects, however the muon's great mass ($\approx 207m_e$) causes some notable differences. One example is that electrons are a factor $(\frac{m_\mu}{m_e})^4$ more likely to undergo Bremsstrahlung while passing through matter, losing energy and hence stopping far faster than muons in matter. Another significant difference is the muons ability to decay via the weak force (Figure 1). The muon's lifetime is an important parameter to particle physicists, as it may be used to determine the value of the Fermi coupling constant G_F, which specifies the strength of the weak interaction.

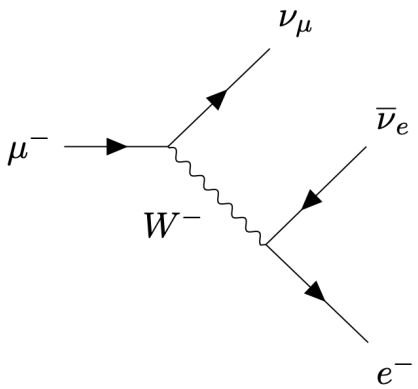

Figure 1: Feynman diagram for muon decay ($\mu \rightarrow e^- + \nu_\mu + \bar{\nu_e}$)

An additional property of the muon worthy of study is the muon's magnetic moment. This quantity is predicted by the Dirac equation to be equal to exactly 2. Experimentally, however, the magnetic moment is found to be slightly greater than this. This is due to contributions from higher order processes causing modifications of the magnetic moment, producing the muon's anomalous magnetic moment a_μ. This quantity acts as a metric for the success of the standard model, as higher order processes may include as yet undiscovered particles. Recent measurements of this value have shown a disagreement between theory and experiment with 4.2σ significance, indicating the likely presence of new physics [1] and demonstrating how valuable the study of the muon is to physics.

Muons and antimuons may be produced through the decay of charged pions ($\pi^+ \rightarrow \mu^+ + \nu_\mu$ and $\pi^- \rightarrow \mu^- + \bar{\nu_\mu}$) produced in particle accelerators such as found in the Paul Scherrer Institute (PSI) [2]. Additionally, muons are produced in cosmic rays - high energy particles (primarily hydrogen and helium nuclei) entering the Earth's atmosphere from above producing showers of subatomic particles (Figure 2). These showers have been studied since 1912 [3], providing the source of high energy particles with which the first antiparticle (the positron) [4], the muon [5] and many other particles were discovered. Cosmic rays have now largely been superseded by particle accelerators in high energy physics (HEP) experiments, however they do still offer interesting insights. Some

cosmic rays have energies that surpass what is currently producible in particle accelerators, such as a particle detected in 1991 with an energy of approximately 320 EeV, (51 Joules) [6], raising questions about their production.

As cosmic muons are so freely available, arriving on Earth at a rate of roughly 1 muon cm^{-2} min^{-1} at sea level [8], they are a perfect tool for education. Detector technology, which is the main drawback to educational studies of cosmic muons, is quickly becoming more accessible and less costly. This topic is particularly relevant to this project and will be discussed in more detail in subsection 2.2. Other examples of muon outreach experiments include the HiSPARC experiment [9], which uses a network of muon detectors located in schools across Europe to study the properties of cosmic rays, and the Extreme Energy Events (EEE) project [10], situated in Italy with similar goals.

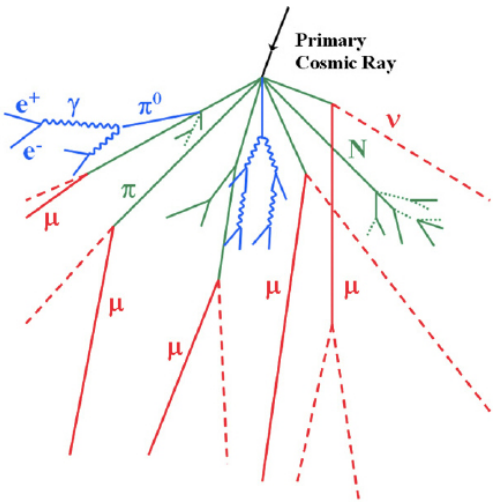

Figure 2: An illustration of a cosmic ray shower adapted from [7]. Particles are shown by different line styles and colours as labelled.

1.2 Monte Carlo simulations

The other major component of this project is Monte Carlo (MC) simulation - the use of programs which utilise the generation of random numbers to model processes. MC techniques are common in HEP as they allow random properties such as particle lifetimes to be modelled and also provide a numerical method for the evaluation of complex integrals. MC simulations are often used prior to experiments to determine expected outcomes, allowing any differences between theory and reality to be determined. Prominent examples of the use of MC simulation in this manner are the muon g-2 experiment [11], as well as the discovery of the Higgs boson [12]. These applications use MC simulators which are optimised for use in HEP such as Geant4 [13] and Pythia [14], having inbuilt particle interactions and sampling tools. Some of these tool-kits are more optimised for the modelling of certain particle interactions or for modelling processes with certain centre-of-mass energies. Due to this, different tool-kits are often used to model different interactions to optimise the reliability of results. As an example, 10 different generators were used to model the different processes involved in the Higgs boson discovery.

For this project, an MC event generator will be created to generate cosmic muons with pseudo-random properties. MC techniques will be used to generate cosmic muons with pseudo-random properties such as energy or zenith angle. While each of these properties are randomly generated, each has a different distribution to be sampled. In order to achieve this, several MC techniques will be employed. The most important of these techniques are the inverse transform method and the acceptance-rejection method, with which almost any given distribution may be sampled using a uniformly distributed random number generator. The inverse transform method relies upon being able to obtain a functional form of the cumulative distribution $F(a) = P(x \leq a) = \int_{-\infty}^{a} f(x)dx$ of the desired probability density function $f(a) = P(x = a)$, and then to be able to find its inverse $F^{-1}(a) = P(a \leq x)$. To generate variables with the desired distribution, simply input a uniformly distributed random variable into the inverse cumulative function $F^{-1}(a)$. If obtaining

$F^{-1}(a)$ is not possible, an alternative sampling method will be required. The acceptance-rejection method requires only that an approximate distribution $Cg(x)$ may be obtained, where $g(x)$ is normalised and easily sampled, e.g. a uniform distribution. C is a scaling constant chosen such that $Cg(x) \geq f(x)$. To generate a point, a candidate x must be generated according to $g(x)$ along with a variable u which is uniformly distributed between 0 and 1. Next, compare the quantities $uCg(x)$ and $f(x)$: if $uCg(x) \leq f(x)$, we may accept x as a valid point. If not, we must reject x and restart the process. The efficiency of this algorithm (the proportion of candidate points which are accepted), is quantified by $1/C = \frac{f(x)}{g(x)}$. To maximise this, $Cg(x)$ should be chosen such that it is as similar to $f(x)$ as possible.

More complex general approaches are also available to sample events. One particularly interesting method is the use of machine learning, where network structures such as generative adversarial networks (GANs) are given real or simulated data which they are trained to mimic. This has previously shown promising results [15], as (once trained) neural networks are far less computationally expensive than most detailed MC simulations and may be optimised to produce satisfactory data. While there are still challenges to overcome in terms of precision, machine learning simulations are very promising and will likely see more use in future MC generators.

2 Muon lifetime

2.1 Research

The most precise measurement of the muon lifetime to date has come from the MuLan collaboration [16], producing a result of $\tau_\mu = (2.1969803 \pm 0.0000022) \times 10^{-6}$s. The principle used in this investigation was the same as most other muon lifetime investigations: produce a large number of muons/anti-muons from a source, measure the time between their production and their decay into an electron/positron, then use the resulting exponential distribution to to extract the lifetime using a functional fit. Anti-muons are used in precision determination of τ_μ rather than muons due to the muons ability to interact with the nuclei of atoms in matter to form muonic atoms. The muon may then interact with a proton in the nucleus via the weak force to produce a neutron and a muon neutrino ($\mu^- + p \rightarrow \nu_\mu + n$). This process causes the measured lifetime of the muon to reduce when in matter, despite the two particles having identical lifetimes when only considering the muon decay process. Anti muons do not undergo this process, making determination of τ_μ simpler when using a beam of only anti-muons.

In this experiment, anti-muons were produced using a beam of positive pions from the πE3 beamline at the PSI. This experiment used an alternating (rather than continuous) beam of μ^+, allowing a single particle detection per muon decay to be made. This improved upon previous muon lifetime experiments such as [18] which required detection of both the parent muon and its daughter positron to determine the lifetime. A sketch of the MuLan setup can be seen in Figure 3. Muons produced by the pion beam were stopped on targets designed to minimise muon precession effects. Muon spin precession can distort the distribution of measured decay times, complicating the measurement of τ_μ. In other experiments such as [18], spin precession effects were dealt with by providing an 80G magnetic field in the target causing rapid precession which may be measured

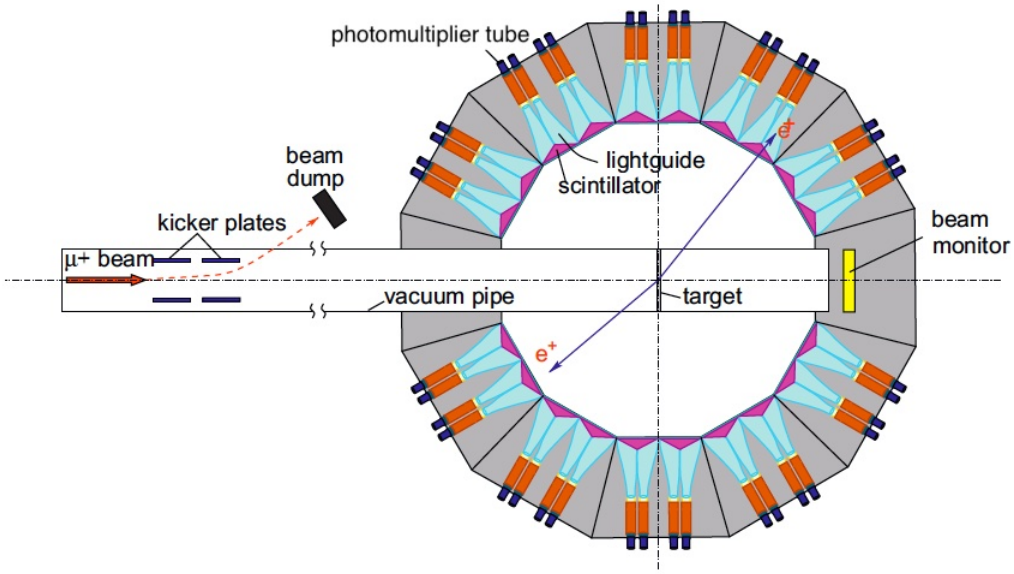

Figure 3: A sketch of the MuLan setup adapted from [17]. For 5μs anti-muons accumulate on the target, then for 22μs the beam is redirected by activating the kicker plates.

and accounted for in analysis.

Data analysis for muon lifetime experiments requires the use of a fit of the form $N(t) = Ne^{t/\tau_\mu} + C$, where N, τ_μ and C are parameters to be fit corresponding to the normalisation, muon lifetime and background respectively. If large spin precession effects are present, additional time-dependent functions to account for this will be required, (e.g., $N(t) = Nf(t)e^{t/\tau} + C$). While the mathematics of this determination is relatively simple, one of the main difficulties with these experiments is the amount of data that must be processed in order to obtain a precise value of τ_μ. As an example, the MuLan experiment required analysis of approximately 1.6×10^{12} decays worth of data. This can be a challenge computationally, particularly when considering storage. Some experiments such as [18] experiment chose to limit the amount of data that must be stored by performing a portion of the data analysis during the experiment, while the MuLan collaboration stores its data physically for analysis later.

2.2 Education

Educational setups for measuring the muon lifetime differ considerably from those found in research. Use of cosmic rays as the muon source removes the need for a particle accelerator to produce pions, meaning only a detector is required. Almost all detectors used for educational muon lifetime experiments follow the same design principles, with the main difference being the data acquisition and readout circuits. Each comprises of a cylindrical block of scintillator connected to one or more photomultiplier tubes. These tubes are connected to a signal amplifier, which then connects to a discriminator which determines if the signal is strong enough to be a particle detection. If the signal is strong enough, a timer begins counting cycles of the inbuilt clock. This timer will stop either when a second particle detection is made before a predetermined timeout time, or when the

clock reaches the timeout time. The first detection is taken to be the time at which a muon enters the detector, and the second is taken to be the time when the muon decays into an electron or positron, making the time between them the measured muon decay time. The setup this project aims to simulate (the TeachSpin muon physics apparatus [19] [20]) uses a 12.7cm tall, 15.2cm diameter cylindrical scintillator connected to a 5.1cm 10-stage bi-alkali (Sb-Rb-Cs and Sb-K-Cs) photomultiplier tube. These components are wrapped in aluminium foil to prevent light leaks and the setup is enclosed within a 36cm tall, 15.2cm diameter aluminium tube capped at both ends to protect the detector. Additionally, an LED is installed near to the scintillator to allow detections to be simulated. A sketch of this setup can be seen in Figure 4.

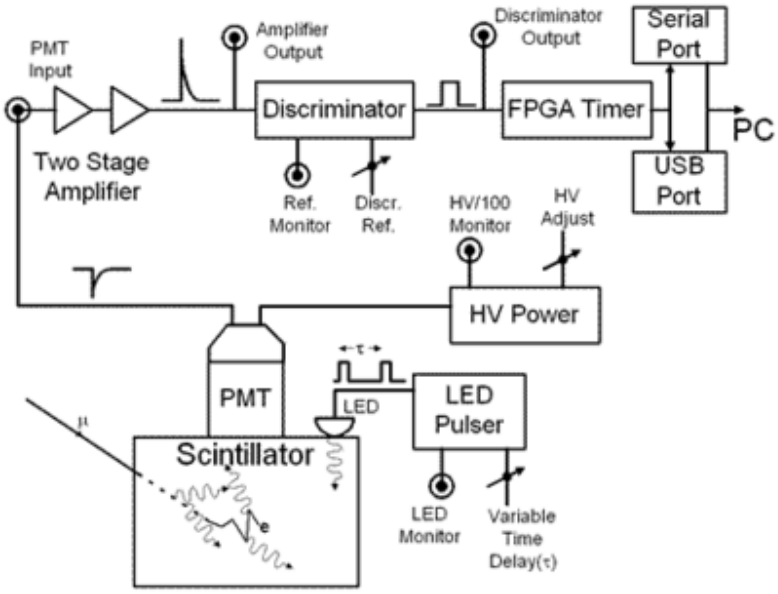

Figure 4: A sketch showing the components of the TeachSpin muon physics apparatus produced by [19].

Generally, detector equipment has been steadily becoming smaller, cheaper and more accessible over time. A detector setup which utilises an oscilloscope (a common piece of equipment in educational physics laboratories) as a signal processor was proposed in 2016, helping to cut costs [21]. Further designs have been investigated which reduce the costs of the signal processing and data acquisition circuits used [22], leading to the main limiting factor of detectors now being the cost and size of the scintillator components. Relatively recently a design for a desktop muon detector composed of small commercially available parts with a total cost of less than US$100 was made available [23]. While somewhat unsophisticated, this setup demonstrates how quickly detector costs are being driven down and the direction that educational muon lifetime setups may be heading.

Similarly to the precision muon lifetime experiments discussed in subsection 2.1, the analysis for educational experiments is relatively simple. Times may be plotted using a histogram, and a fit may be made using the form $N(t) = Ne^{t/\tau_\mu} + C$. One complication is the presence of both muons and anti-muons in the detection sample which, as discussed in subsection 2.1, will cause the measured muon lifetime to be reduced. If enough data is collected, the lifetime of the anti-muon and the effective lifetime of the negative muon may be resolved during analysis through use of a fit such as $N(t) = N_1e^{t/\tau_+} + N_2e^{t/\tau_-} + C$ where τ_+ and τ_- are the lifetimes of the anti-muon and

muon respectively.

3 Outline

This project aims to use Python to produce a detailed Monte Carlo simulation of the TeachSpin Muon Physics detector described in [19]. Additionally, an analysis framework for the results of the simulation will be produced for quick interpretation of the results. The project may be viewed as three broad sections: modelling of cosmic muons, modelling of the detector and environment, and the analysis framework. An approximate timeline for the project is shown in Table 1.

Target completion date	**Simulation feature**
8$^{\text{th}}$ November 2021	Muon/anti-muon lifetime distributions and zenith angle distributions.
22$^{\text{nd}}$ November 2021	Muon energy distribution and energy loss.
6$^{\text{th}}$ December 2021	Detector geometry and determination of muons hitting or missing the detector. Determination of muons stopping in the detector and path length calculation.
17$^{\text{th}}$ January 2022	Detector start/stop/timeout system.
31$^{\text{st}}$ January 2022	Analysis tools.
14$^{\text{th}}$ February 2022	Treating multiple muons entering the detector.
28$^{\text{th}}$ February 2022	Correlation of energy and angular distribution. Increased level of detail on energy loss algorithm.
7$^{\text{th}}$ March 2022	Detector background detections.
21$^{\text{st}}$ March 2022	Performance optimisation.

Table 1: Estimated project timeline

Muons will be generated with pseudo-random properties using the techniques outlined in subsection 1.2. This will include an approach angle to the detector, the initial muon energy, production position and muon charge (+/-). The zenith approach angle to the detector will be generated according to the distribution $I(\theta) = I_0 \cos^2(\theta)$, where I_0 is the muon flux at zenith angle $\theta = 0$ [24]. This will be combined with the initial position of the muon to determine if muons hit the detector. The initial energy of each muon will be generated according to the distributions described in [25]. The Bethe-Bloch formula will be applied iteratively to determine if a muon stops in the detector, allowing its lifetime to be measured. The lifetimes of each muon will be generated according to an exponential distribution with rate parameter $\frac{1}{\tau_\mu}$, where τ_μ is the lifetime of the muon or antimuon.

The other key aspect of the project is simulation of the detector setup. The geometry of the detector will be specified and allowed to change, allowing for analysis of dependencies upon detector scale. A start, stop and timeout algorithm will be implemented to determine decay times and allow instances of multiple muons entering the detector at once to be treated. An additional part of the simulation is background detections due to sources of ionising radiation. This will require the introduction of noise in the system, possibly increasing the number of events required to resolve the muon lifetimes.

The final aspect of the project is the analysis framework. This framework will allow useful information to be extracted from the data produced by the simulation. This section of the project is more open ended, however the main aims are algorithms to determine the number of muon detections required to resolve the muon and antimuon lifetimes, as well as algorithms to determine how the simulation depends upon the detector parameters (e.g., timeout time, detector geometry, sampling time etc.).

References

[1] B. Abi *et al.*, "Measurement of the Positive Muon Anomalous Magnetic Moment to 0.46 ppm," *Phys. Rev. Lett.*, vol. 126, no. 14, Apr. 2021. DOI: 10.1103/PhysRevLett.126.141801. arXiv: 2104.03281.

[2] R. Abela *et al.*, "Muon beams at PSI," *Zeitschrift für Phys. C Part. Fields*, vol. 56, no. 1 Supplement, S240–S242, Mar. 1992. DOI: 10.1007/BF02426803. [Online]. Available: https://link.springer.com/article/10.1007/BF02426803.

[3] V. Hess, "On the Observations of the Penetrating Radiation during Seven Balloon Flights," *Phys. Zeitschrift 13*, pp. 1084–1091, Jul. 2018. arXiv: 1808.02927. [Online]. Available: http://arxiv.org/abs/1808.02927.

[4] C. D. Anderson *et al.*, *Positrons from gamma-rays*, Jun. 1933. DOI: 10.1103/PhysRev.43.1034. [Online]. Available: https://journals-aps-org.libproxy.ucl.ac.uk/pr/abstract/10.1103/PhysRev.43.1034.

[5] S. H. Neddermeyer *et al.*, "Note on the nature of cosmic-ray particles," *Phys. Rev.*, vol. 51, no. 10, pp. 884–886, May 1937. DOI: 10.1103/PhysRev.51.884. [Online]. Available: https://journals-aps-org.libproxy.ucl.ac.uk/pr/abstract/10.1103/PhysRev.51.884.

[6] D. J. Bird *et al.*, "Detection of a cosmic ray with measured energy well beyond the expected spectral cutoff due to cosmic microwave radiation," *Astrophys. J.*, vol. 441, p. 144, Oct. 1995. DOI: 10.1086/175344. arXiv: 9410067 [astro-ph]. [Online]. Available: https://arxiv.org/abs/astro-ph/9410067v1.

[7] F. Blanco *et al.*, "Cosmic rays with portable Geiger counters: From sea level to airplane cruise altitudes," *Eur. J. Phys.*, vol. 30, no. 4, pp. 685–695, May 2009. DOI: 10.1088/0143-0807/30/4/003. [Online]. Available: https://iopscience.iop.org/article/10.1088/0143-0807/30/4/003https://iopscience.iop.org/article/10.1088/0143-0807/30/4/003/meta.

[8] P. A. Zyla *et al.*, *Review of particle physics*, Aug. 2020. DOI: 10.1093/ptep/ptaa104. [Online]. Available: https://academic.oup.com/ptep/article/2020/8/083C01/5891211.

[9] B. van Eijk *et al.*, "Public Awareness Activities: HISPARC: A Joint Venture for Research and Education," *Nucl. Phys. News*, vol. 15, no. 2, pp. 45–49, Apr. 2005. DOI: 10.1080/10506890500454741. [Online]. Available: https://www.tandfonline.com/doi/abs/10.1080/10506890500454741.

[10] M. Abbrescia *et al.*, "Operation and performance of the EEE network array for the detection of cosmic rays," *Nucl. Instruments Methods Phys. Res. Sect. A Accel. Spectrometers, Detect. Assoc. Equip.*, vol. 845, pp. 383–386, Feb. 2017. DOI: 10.1016/j.nima.2016.05.112. [Online]. Available: https://linkinghub.elsevier.com/retrieve/pii/S0168900216305150.

[11] T. Albahri *et al.*, "Measurement of the anomalous precession frequency of the muon in the Fermilab Muon g-2 Experiment," *Phys. Rev. D*, vol. 103, no. 7, Apr. 2021. DOI: 10.1103/PhysRevD.103.072002. arXiv: 2104.03247.

[12] G. Aad *et al.*, "Observation of a new particle in the search for the Standard Model Higgs boson with the ATLAS detector at the LHC," *Phys. Lett. B*, vol. 716, no. 1, pp. 1–29, Sep. 2012. DOI: 10.1016/J.PHYSLETB.2012.08.020.

[13] CERN, *Overview | geant4.web.cern.ch*. [Online]. Available: https://geant4.web.cern.ch/ (visited on 09/30/2021).

[14] T. Sjöstrand *et al.*, "An introduction to PYTHIA 8.2," *Comput. Phys. Commun.*, vol. 191, no. 1, pp. 159–177, 2015. DOI: 10.1016/j.cpc.2015.01.024. arXiv: 1410.3012.

[15] M. Paganini *et al.*, "Accelerating Science with Generative Adversarial Networks: An Application to 3D Particle Showers in Multilayer Calorimeters," *Phys. Rev. Lett.*, vol. 120, no. 4, p. 042 003, Jan. 2018. DOI: 10.1103/PhysRevLett.120.042003. arXiv: 1705.02355. [Online]. Available: https://arxiv.org/abs/1705.02355v2https://link.aps.org/doi/10.1103/PhysRevLett.120.042003.

[16] R. Carey *et al.*, "Mulan: a part-per-million measurement of the muon lifetime and determination of the Fermi constant," Aug. 2021. arXiv: 2108.09182. [Online]. Available: http://arxiv.org/abs/2108.09182.

[17] V. Tishchenko *et al.*, "Data acquisition system for the MuLan muon lifetime experiment," *Nucl. Instruments Methods Phys. Res. Sect. A Accel. Spectrometers, Detect. Assoc. Equip.*, vol. 592, no. 1-2, pp. 114–122, Jul. 2008. DOI: 10.1016/j.nima.2008.03.121.

[18] A. Barczyk *et al.*, "Measurement of the Fermi constant by FAST," *Phys. Lett. Sect. B Nucl. Elem. Part. High-Energy Phys.*, vol. 663, no. 3, pp. 172–180, Jul. 2008. DOI: 10.1016/j.physletb.2008.04.006. arXiv: 0707.3904. [Online]. Available: https://arxiv.org/abs/0707.3904v2.

[19] TeachSpin Inc., *Muon Physics | TeachSpin*. [Online]. Available: https://www.teachspin.com/muon-physics (visited on 10/30/2021).

[20] T. Coan *et al.*, "A compact apparatus for muon lifetime measurement and time dilation demonstration in the undergraduate laboratory," *Am. J. Phys.*, vol. 74, no. 2, pp. 161–164, Feb. 2006. DOI: 10.1119/1.2135319. arXiv: 0502103 [physics]. [Online]. Available: https://arxiv.org/abs/physics/0502103v1.

[21] Y. Hu *et al.*, "A simple setup to measure muon lifetime and electron energy spectrum of muon decay and its Monte Carlo simulation," vol. 2, no. August, Aug. 2016. arXiv: 1608.06936. [Online]. Available: http://arxiv.org/abs/1608.06936.

[22] D. Bosnar *et al.*, "A simple setup for cosmic muon lifetime measurements," *Eur. J. Phys.*, vol. 39, no. 4, Jan. 2018. DOI: 10.1088/1361-6404/aaadec. arXiv: 1801.07219. [Online]. Available: https://arxiv.org/abs/1801.07219v1.

[23] S. N. Axani *et al.*, "The CosmicWatch Desktop Muon Detector: A self-contained, pocket sized particle detector," *J. Instrum.*, vol. 13, no. 3, P03019, Mar. 2018. DOI: 10.1088/1748-0221/13/03/P03019. arXiv: 1801.03029. [Online]. Available: https://iopscience.iop.org/article/10.1088/1748-0221/13/03/P03019.

[24] P. Shukla *et al.*, "Energy and angular distributions of atmospheric muons at the Earth," *Int. J. Mod. Phys. A*, vol. 33, no. 30, Jun. 2018. DOI: 10.1142/S0217751X18501750. arXiv: 1606.06907. [Online]. Available: http://arxiv.org/abs/1606.06907.

[25] P. Achard *et al.*, "Measurement of the atmospheric muon spectrum from 20 to 3000 GeV," *Phys. Lett. B*, vol. 598, no. 1-2, pp. 15–32, Sep. 2004. DOI: 10.1016/J.PHYSLETB.2004.08.003.